X Rays

November 1, 2016

Author: Jacob Cluff

Partners: Josef Rinderer, David Turk

Abstract:
In this experiment, X-ray spectra, emission and absorption lines, and bragg diffraction are explored. The Mosley fitting parameters, C and σ for the $K_{1,2}$ series are found to be $.01049 \pm 2.391 \times 10^{-4}$ and $.9972 \pm .1270$. The power fitting parameter used to find K_β doublets is found to be $n = 3.968 \pm .04300$. The most prominent absorption edge is found to be $\approx 17.4\ keV$. Other prominent results can be found in the appendix.

Introduction:

X-rays are created when high energy sources strike a target. Each element has characteristic emission/absorption lines that correspond with differences between energy levels of the specific target. Each element has a unique spectra, similar to a fingerprint.

The Bohr model gives a basic understanding of energy levels for hydrogen like atoms (one electron orbiting a positively charged nucleus). In many cases, this is only a rough approximation. In reality, there tend to be many electrons orbiting the nucleus, none of which can share the same four quantum numbers describing shell, angular momentum, magnetic moment, and spin. All these electrons have complex interactions that tend to push electrons in tighter orbits closer to the nucleus and push electrons in outer orbits away. This complex behavior gives an effective charge (Z_{eff}) to the nucleus. This explanation gives a physical motivation behind Mosley's Law (Equation 4), where C and σ are constants found for each series.

When energetic electrons (< 50 keV) are quickly decelerated, they emit bremsstrahlung radiation perpendicular to the deceleration vector. The bremsstrahlung radiation has a continuous spectrum starting with a minimum wavelength. The highly energetic electrons burrow deep into the target atom and knock out electrons from inner orbitals. When electrons from outer shells transition to the vacancy, they emit photons, causing emission lines in the bremsstrahlung continuous spectrum. Using Bragg diffraction, it is possible to determine the energies of various transitions.

Theory:

Equation 1 is used to transform the channel measured to keV.

$$\begin{aligned} x' &= A + Bx \\ A &= x'_1 - \left(\frac{x'_2 - x'_1}{x_2 - x_1}\right) x_1 \\ B &= \frac{x'_2 - x'_1}{x_2 - x_1} \\ x_1 &= \text{channel of Cu } K_\alpha = 270 \\ x'_1 &= \text{Cu } K_\alpha = 8.04 \ keV \\ x_2 &= \text{channel of } {}^{241}\text{Am} = 1970 \\ x'_2 &= {}^{241}\text{Am} = 59.5 \ keV \end{aligned} \tag{1}$$

Equation 2 gives the Bohr energy, which is used for hydrogen like atoms (one electron orbiting a nucleus) or to roughly approximate transition energies for non-hydrogen like atoms.

$$\begin{aligned} \Delta E_{Bohr} &= \mathcal{R} Z^2 \left(\frac{1}{m^2} - \frac{1}{n^2}\right) \\ \mathcal{R} &= \text{Rydberg constant} = 13.6 \ eV \\ Z &= \text{atomic number} \\ m \to n &= \text{transition} \end{aligned} \tag{2}$$

Equation 3 is Mosley's law, where C and σ are constants found for a specific series.

$$E(Z) = C(Z - \sigma)^2 \tag{3}$$

Equation 4 gives an approximation of the difference in energies between the K_β line and its doublet.

$$\Delta E_{so} \sim Z^4 \tag{4}$$

Equation 5 describes the intensity attenuation from a element with mass density ρ, thickness x, and absorption coefficient $\mu(E_\gamma)$.

$$\begin{aligned} I_0 e^{x/\lambda} &= I_0 e^{-\mu(E_\gamma)\rho x} \\ \Rightarrow \frac{-x}{\lambda} &= -\mu(E_\gamma)\rho x \\ \Rightarrow \mu(E_\gamma) &= \frac{1}{\rho\lambda} \end{aligned} \tag{5}$$

Equation 6 gives the error propagation of μ.

$$\delta\mu = \frac{\delta\lambda}{\rho\lambda^2} \tag{6}$$

Equation 7 gives a power law for the absorption coefficient that is strongly energy dependent.

$$\mu(E_\gamma) = E_\gamma^{-n} \tag{7}$$

Equation 8 is Bragg's diffraction equation where n = 0, 1, 2, ..., λ is the wavelength of light, d is the separation of the crystal's lattice planes, h is Planck's constant, c is the speed of light, and E_γ is the energy of the radiation.

$$\begin{aligned} n\lambda &= 2d\sin\theta \\ E_\gamma &= h\nu = \frac{hc}{\lambda} \\ \Rightarrow \theta &= \arcsin\left(\frac{n\ hc}{2dE_\gamma}\right) \end{aligned} \tag{8}$$

Procedure:

After setting up the Multi-Channel Analyzer (MCA), the Cu source is placed in front of detector in such a way as to eliminate as much dead space as possible, but enough room to fit the Zr foils later on and still keep the source in the same position; about 1 dm directly in front of the detector should be sufficient.

At this point, it is customary to calibrate the axis by carefully selecting the peaks of the Cu K_α and ^{241}Am lines and entering in their respective energies. This calibration transforms the channel number into keV using Equation 1. Although this step is taken, a more accurate calibration is achieved during data analysis. As seen in Figure 1, a vertical line is plotted against the spectra and manually adjusted to get the best determination of the peak. The results of this calibration are found in Table 1, located in the Appendix.

At this point, Cu is replaced with a stronger source and counting statistics are done. Ten, ten second measurements are taken and the average and σ_1 values are calculated. Next, one ninety second measurement is taken. With only one measurement, it is impossible to take an average or standard

deviation so a Poisson error is considered instead. The Poisson error is calculated using $\sqrt{N}$ or $\sqrt{CPS}$ (Counts Per Second) and is compared with the average and standard deviation of the 10 shorter measurements. The results of this exercise are found in Figure 12 in the Appendix.

Now, spectra of all the samples are taken. In order to get the best readings, the data is allowed to collect for a minute for each sample. The data is then plotted along with vertical lines corresponding with the K_α and ^{241}Am line. These vertical lines are designed to test the accuracy of the new calibration.[1]

Mosley's law is now used to calculate the K_α line for each sample. Parameters C and σ are fitted to Equation 3 using an algorithm that goes through a progressive series that narrows down the values and returns the parameters that give the smallest absolute magnitude of difference with the known Energy.[2]

The spin orbit interaction is now explored. The spectra are plotted focused on the K_β region. It is found that only Ag, Ba, and Tb show obvious spin-orbit doublets. A similar fitting algorithm as the one used to find the Mosley fits is used to find the "n" power that returns the lowest error.[3]

Next, attenuation is explored by using various thicknesses of Zr foil against a single Mo source. The resulting spectra are plotted along with two vertical lines showing the Zr K_β and doublet lines. The two Zr lines show that the Mo K_α line is expected to have particularly strong attenuation.[4]

Equation 5 is then fitted for each spectra in the sample using only Zr foil thickness of .04 inches. λ is then fitted to each spectra. A horizontal line is plotted for each spectra that predicts the resulting spectral density.[5] Finally, the λ parameters found are then used to calculate the absorption coefficient, μ, from Equation 5.[6]

An absorption edge is found by collecting all known energy and intensities. All of the K_α, K_β, and spin orbit doublets for Mo are collected into a single array and plotted. When looking for an absorption edge, a sharp drop off in attenuation is expected, followed by a steady rise.[7]

Next, the X-ray apparatus discussed in "Leybold Document" is used to explore Bragg diffraction using a salt crystal. First, appropriate parameters are set to get clean data. ΔB, B_{min}, B_{max}, Δt, I_{source}, and U are set to .1 degrees, 2.5 degrees, 30 degrees, 10 seconds, 0.1 mA, and 35 keV. Mo and W measurements are taken without a Zr attenuation cap, then taken with the Zr attenuation cap. These four measurements are compared together.[8] Equation 8 is used to plot the first three Bragg diffraction scattering angles using the K_α and K_β energies. Since the K_α and K_β energies of W are above the 35 keV threshold, they will not appear as emission lines; however, Equation 2 is used to calculate likely energies to to appear. The most likely energy found is $K_{2,3}$.[9]

Finally, a comparison is made between different U. B_{min} and B_{max} are changed to 3 and 12.5 degrees and U is lowered to 30 keV. The resulting spectrum is then compared with U = 35 keV over the same range.[10]

[1] See Figure 2 in Results
[2] See Figure 3 (Results) and Table 2 (Appendix)
[3] See Figure 4 and Figure 5 (Results) and Table 3 (Appendix)
[4] See Figure 6 (Results)
[5] See Figure 7 (Results) and Table 4 (Appendix)
[6] See Table 5 (Appendix)
[7] See Figure 9 (Results) and Table 6 (Appendix)
[8] See Figure 10 (Results)
[9] See Table 7 (Appendix)
[10] See Figure 11 (Result). Additional measurements at U = 25 keV and U = 20 keV were desired, but were not taken due to software issues and lack of time.

Results:

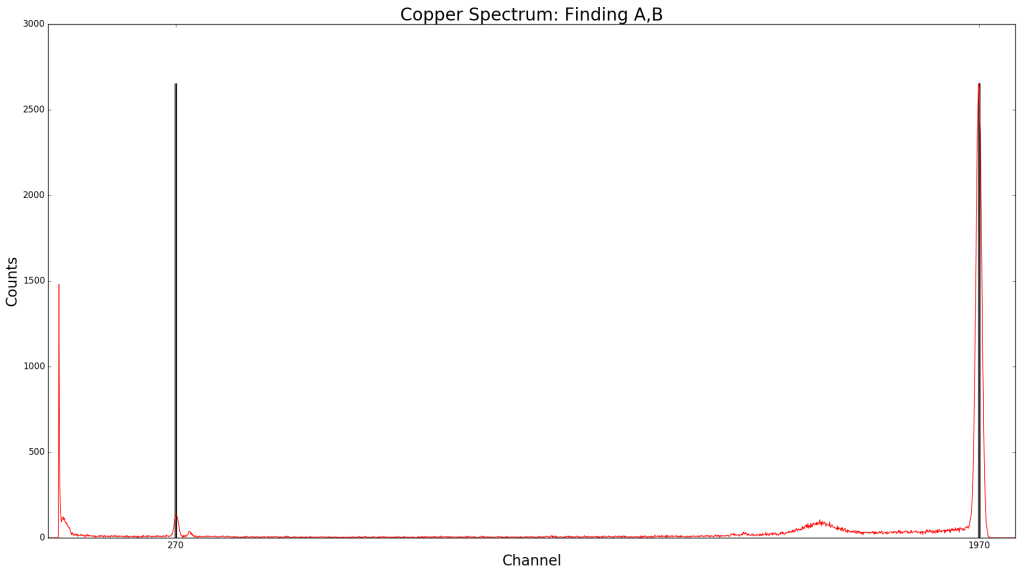

Figure 1: The red curve shows the Cu spectrum and the black vertical lines show the peaks of Cu K_α and ^{241}Am lined up by eye with their respective channel displayed beneath. The fitting parameters are found in Table 1 in the appendix.

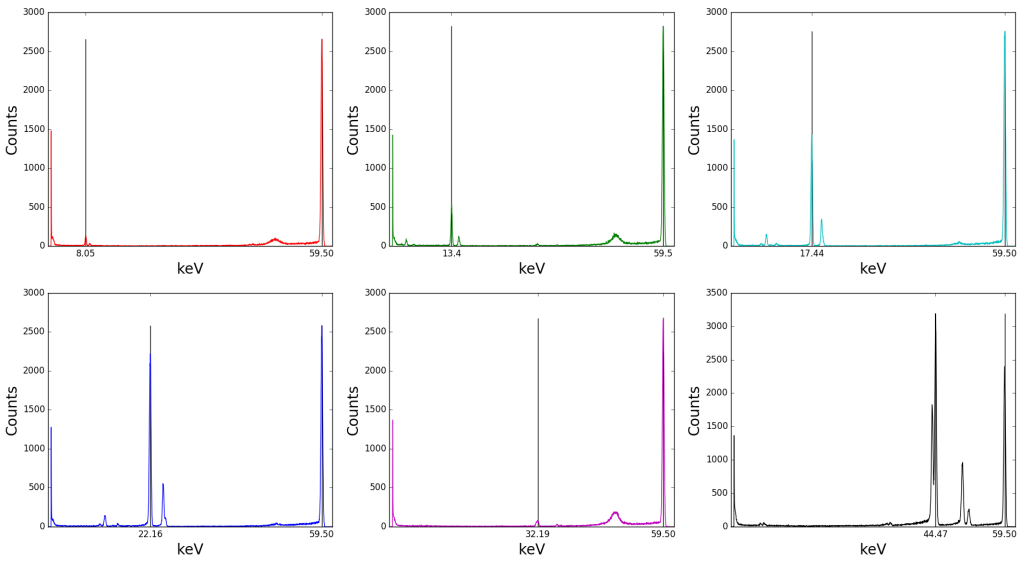

Figure 2: The spectra for each element in the sample wheel are shown with the Cu K_α and ^{241}Am peaks lined up with their respective energies displayed beneath. This figure shows the accuracy of the channel $\rightarrow$ keV conversion.

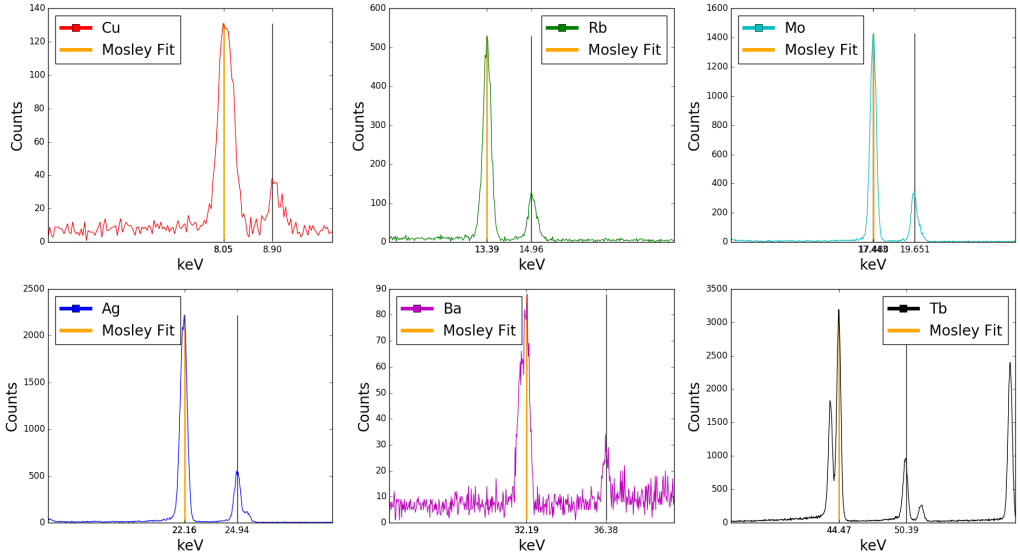

Figure 3: The spectra for each element are shown in the localized region of the K_α and the K_β lines. The orange vertical lines show the Mosley fits from Equation 3 while the black vertical lines show the K_β lines. The values for C are found to be 0.01049 ± 0.0002391, σ is found to be 0.9972 ± 0.1270. More details on the fitting parameters are found in Table 2 in the appendix.

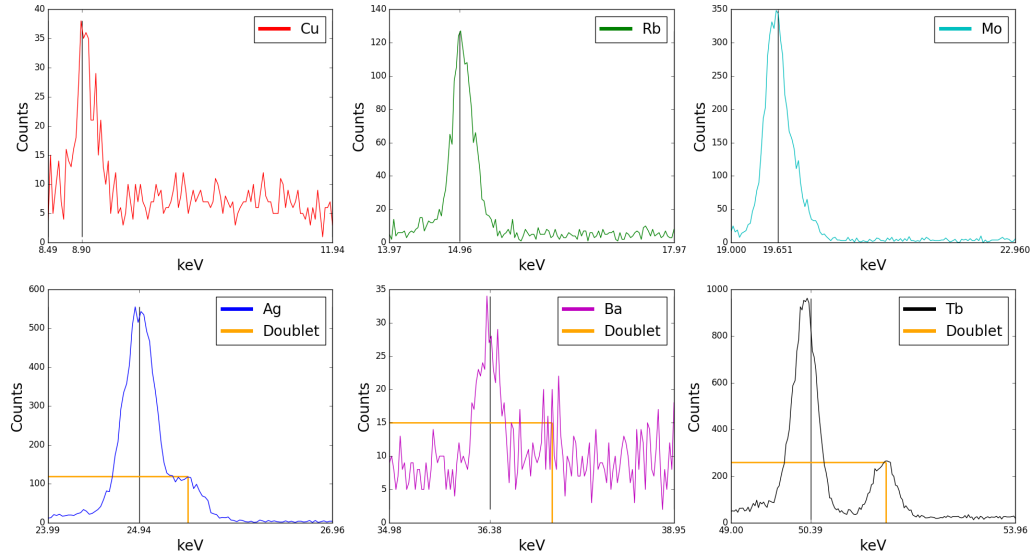

Figure 4: The top three plots do not show an obvious K_β doublet. The bottom three plots show vertical and horizontal orange lines, which are manually adjusted to fit the peak.

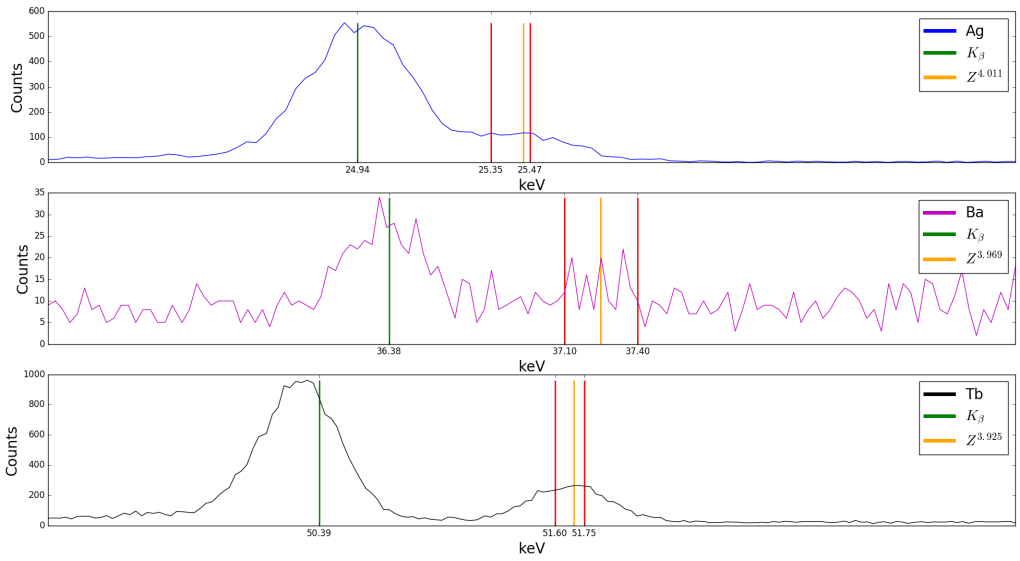

Figure 5: The three plots from Figure 4 that show the K_β doublet are splayed out for further analysis. The green lines show the K_β lines, the red bounds show the region where the doublet is expected to appear, and the orange lines show $K_\beta + E_{so}$ which is found by fitting Equation 4 for Z^{-n}. It is found that $n = 3.968 \pm .04300$; further results are shown in Table 3 in the appendix.

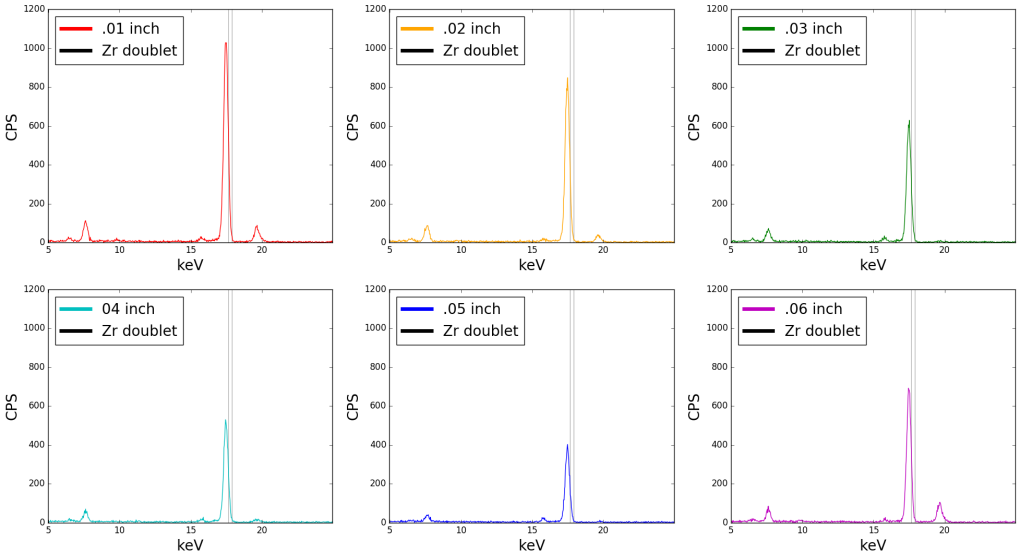

Figure 6: These six plots show the Mo region in the localized region of Mo K_α and K_β. The two black vertical lines show the Zr β and β doublet lines, which suggests that Mo $K\alpha$ will be strongly attenuated. The attenuation of the Mo spectra is plain to see as the Zr thickness increases.

The last plot in Figure 3 (.06 inch Zr foil thickness) gives a confusing result. The CPS is clearly attenuated, but shows an attenuation level somewhere between .02 and .03 thickness. However, the Mo K_β line shows no obvious attenuation. This result clearly shows that it was attenuated by the Zr foil, and that it was not merely mixed up with other data (because of the β line). This result is not fully understood and could be the effect of misaligned foils or some other user error. In order to better understand this result, the same measurement would have to be taken again, taking extra care to make sure it is set up correctly and see how the new measurement compares with the previous.

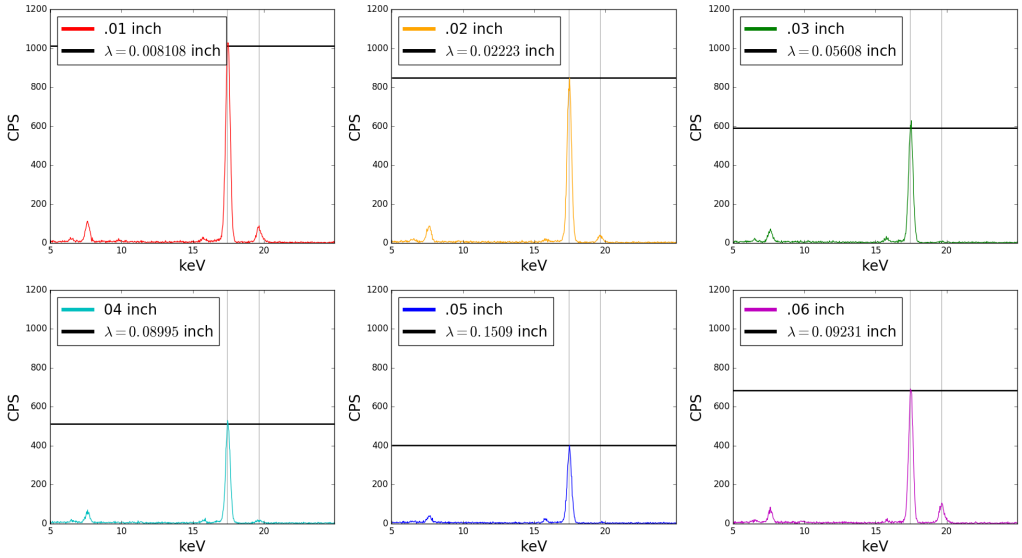

Figure 7: The black horizontal lines in these plots show the resulting CPS after the Mo is attenuated by various thicknesses of Zr. The attenuation is found by fitting Equation 5 with λ. More detailed information found in the Appendix (Table 4).

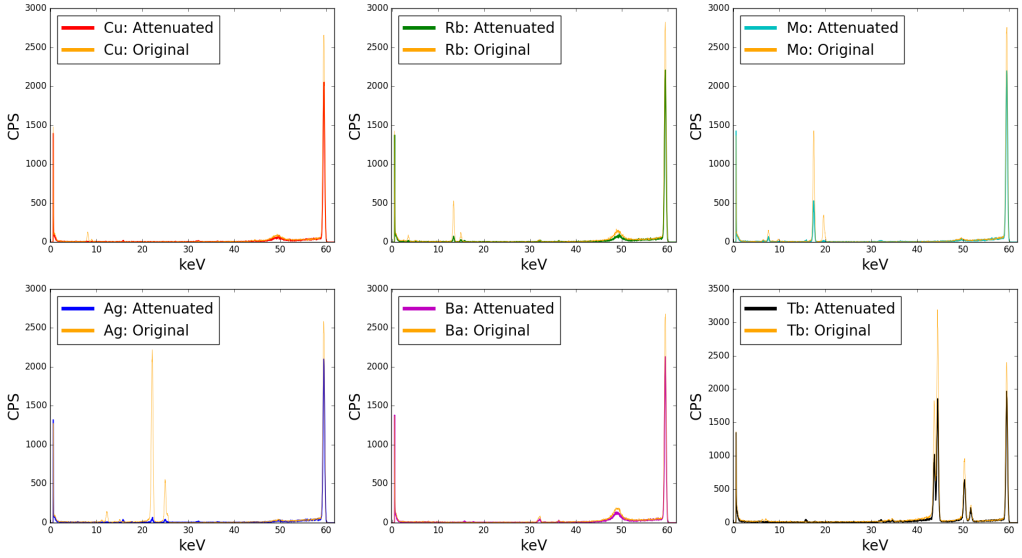

Figure 8: These plots compare the attenuated spectra to the corresponding non-attenuated spectra (yellow).

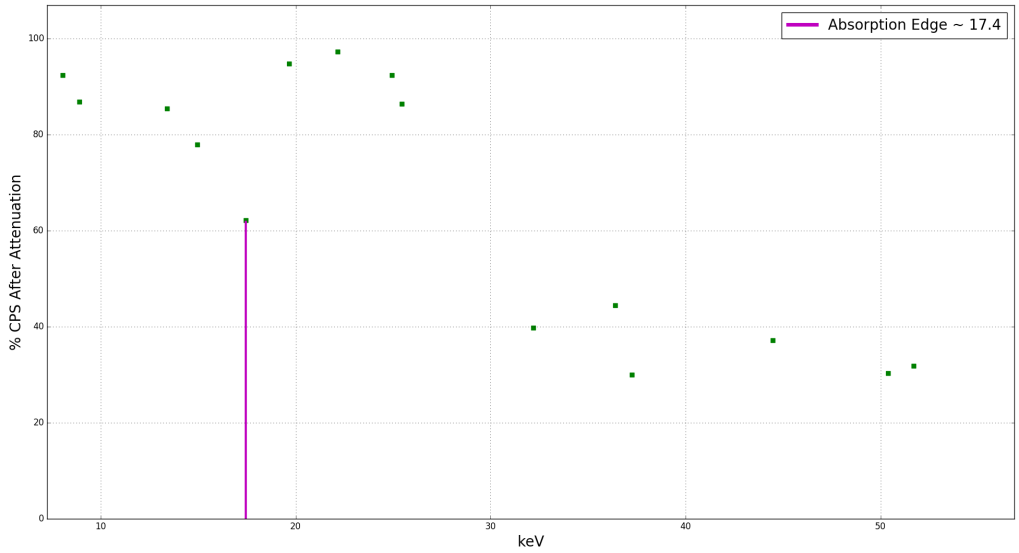

Figure 9: This plot shows the percentage of the remaining CPS after attenuation for all available energies. There seems to be a sharp drop around $keV = 17.43$, which corresponds with the K_α line.

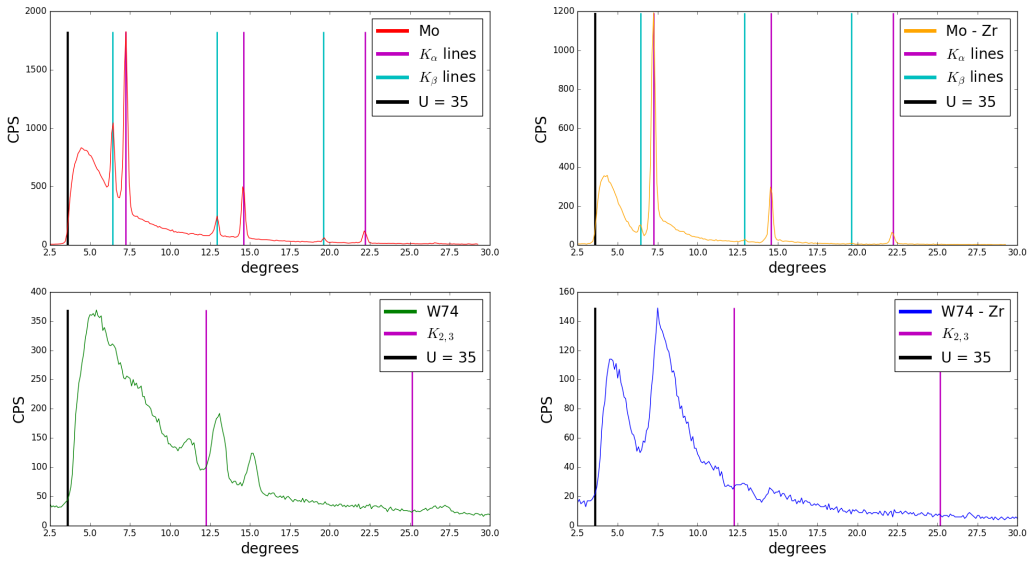

Figure 10: This figure compares both Mo to W74 sources and Zr-filtered to not-filtered X-ray spectra. The strong black line represents the energy cutoff at $U = 35\ keV$. For Mo, the magenta and cyan lines show the alpha and beta lines. For W74, the $K_{2,3}$ energy is approximated using the Bohr energy (Equation 2). It is noticed that there is strong absorption around 6 degrees on Tungsten, which possibly corresponds with an absorption edge. The transition energies and Equation 8 are used to compute the peak angles.

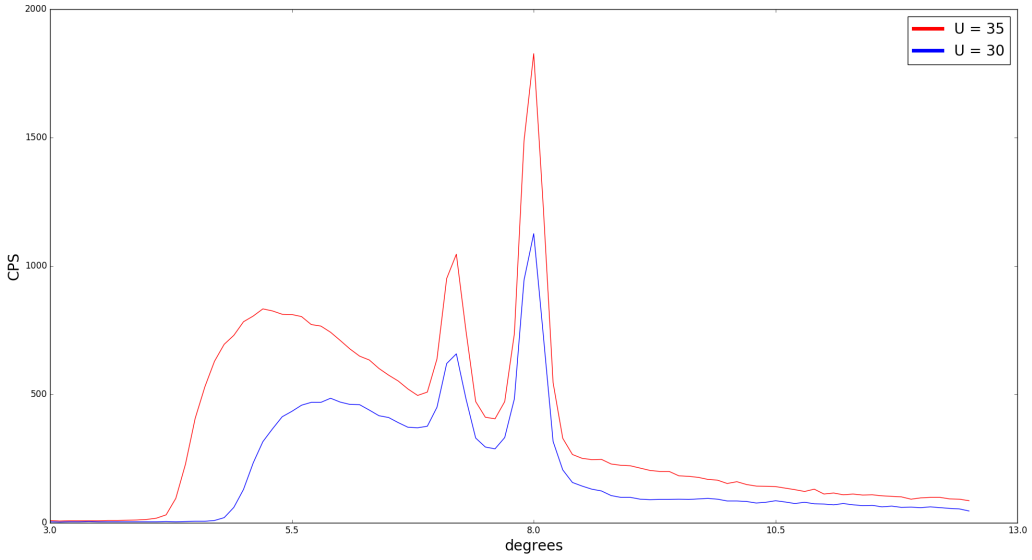

Figure 11: This compares the X-ray spectra from a Mo source when U is varied and shows that the CPS drastically decreases as U decreases. As long as U is greater than the energy of the emission line, the emission line will appear. As $U \to E_{emission}$, $CPS_{emission} \to 0$.

Appendix:

Table 1: Calibrating Software

Fitting Channels		Fitting Parameters	
Cu K_α	^{241}Am	A	B
270	1970	-0.133	0.03027

Ba	10										Average	STD
actual time	10.16	10.59	10.61	10.69	10.03	10.69	10.11	10.62	10.07	10.23	10.38	0.2807
alpha	825	942	715	819	928	829	855	847	824	848	843.2	62.41
beta	214	160	74	122	131	181	151	168	223	108	153.2	46.42
weighted time	1.016	1.059	1.061	1.069	1.003	1.069	1.011	1.062	1.007	1.023	1.038	0.02807
weighted alpha	838.2	997.578	758.615	875.511	930.784	886.201	864.405	899.514	829.768	867.504	874.808	63.23
weighted beta	217.424	169.44	78.514	130.418	131.393	193.489	152.661	178.416	224.561	110.484	158.68	46.95
cps alpha	81.2	88.95	67.39	76.61	92.52	77.55	84.57	79.76	81.83	82.89	81.33	6.91
cps beta	21.06	15.11	6.97	11.41	13.06	16.93	14.94	15.82	22.14	10.56	14.8	4.63

Ba	100 sec	sqrt(N)	compare 10 sec to 100 sec with regular std		
actual time	90.5		total	std	Difference
alpha	7507	86.64	7917	572.2	410
beta	1285	35.85	1436	424.9	151.1
Ba	CPS	sqrt(CPS)	CPS	std	Difference
alpha	82.95	9.108	81.33	6.912	1.6
beta	14.2	3.768	14.8	4.626	0.6

Figure 12: Counting Statistics

Table 2: Mosley Fits

Element	$E_{min}keV$	$E_{max}keV$	C	σ	E_α	δE_α
Cu	5	10	0.01023	0.9444	8.050	2.177e-7
Rb	10	20	0.01036	1.046	13.39	2.778e-6
Mo	10	25	0.01031	0.8303	17.48	6.629e-7
Ag	15	30	0.01041	.8644	22.16	9.655e-7
Ba	25	40	0.01070	1.144	32.19	9.084e-6
Tb	35	60	.01091	1.155	44.47	9.289e-6
		Average	.01049	.9972		
		σ_1	2.391e-4	.1270		

Table 3: Doublet Fits

Element	E_{eye} keV	CPS	ΔE_{eye} keV	ΔCPS_{eye}	n_{fit}	E_{fit} keV	ΔE_{fit} %
Cu	no visual doublet						
Rb	no visual doublet						
Mo	no visual doublet						
Ag	25.45	120	0.005	5	4.011	25.449	0.1765 %
Ba	37.25	15	.005	.5	3.969	37.248	0.2335 %
Tb	51.7	260	.05	5	3.925	51.695	0.3958 %
				Average	3.968		
				σ_1	0.04300		

Table 4: λ Fits

x (inch)	λ_{fit} $inch$	Attenuation (CPS)	CPS_{model}	δ CPS	δ CPS %
.01	8.108e-3	416.3	1013	14.3	1.412
.02	2.223e-2	581	848	2.525e-3	2.978e-4
.03	5.608e-2	837	592	3.679e-2	6.214e-4
.04	8.995e-2	916	513	1.361e-3	2.653e-4
.05	.1509	1026	403	3.25e-2	8.066e-3
.06	9.231e-2	746	683	8.95e-3	1.31e-3

Table 5: Finding μ

x (inch)	μ (cm^2/g)	$\Delta\mu$ (cm^2/g)
.01	7.54	33780
.02	2.75	.7934
.03	1.09	1.816
.04	0.6796	0.02612
.05	0.4051	0.2216
.06	0.6622	0.1631

Table 6: Absorption Edge Data

keV	CPS	Attenuated CPS	% Remaining
8.05	131	10	92.4
8.90	38	5	86.8
13.39	529	77	85.4
14.96	127	28	78.0
17.443	1402	530	62.2
19.651	343	18	94.8
22.16	2220	61	97.3
24.94	515	39	92.4
25.45	118	16	86.4
32.19	83	50	39.8
36.38	27	15	44.4
37.25	20	14	30
44.47	2957	1857	37.2
50.39	845	589	30.3
51.7	264	180	31.8

Table 7: Bragg θ

Element	E	θ_1 degree	θ_2 degree	θ_3 degree
Mo	K_α	7.24	14.6	22.2
	K_β	6.42	12.9	19.6
W74	$K_{2,3}$	12.3	25.2	39.6

All results, data, and program code are available upon request at
<https://drive.google.com/drive/folders/0BzjQ_RadlQmdUVZPUGh4b1IyNUU>